A Hybrid Stochastic/Interval Approach to Transmission-Constrained Unit Commitment

Yury Dvorkin, *Student Member, IEEE*, Hrvoje Pandžić, *Member, IEEE*, Miguel A. Ortega-Vazquez, *Member, IEEE*, and Daniel S. Kirschen, *Fellow, IEEE*

***Abstract*—This paper proposes a new transmission-constrained unit commitment method that combines the cost-efficient but computationally demanding stochastic optimization and the expensive but tractable interval optimization techniques to manage uncertainty on the expected net load. The proposed hybrid unit commitment approach applies the stochastic formulation to the initial operating hours of the optimization horizon, during which the wind forecasts are more accurate, and then switches to the interval formulation for the remaining hours. The switching time is optimized to balance the cost of unhedged uncertainty from the stochastic unit commitment against the cost of the security premium of the interval unit commitment formulation. These hybrid, stochastic, and interval formulations are compared using Monte Carlo simulations on a modified 24-bus IEEE Reliability Test System. The results demonstrate that the proposed unit commitment formulation results in the least expensive day-ahead schedule among all formulations and can be solved in the same amount of time as a full stochastic unit commitment. However, if the range of the switching time is reduced, the hybrid formulation in the parallel computing implementation outperforms the stochastic formulation in terms of computing time.**

***Index Terms*—Interval optimization, stochastic optimization, uncertainty, unit commitment.**

I. Introduction

MODERN power systems accommodate substantial amounts of intermittent energy resources, such as wind and solar generation, which cause uncertainty on the net load, i.e., the load that must be served by conventional generation. To alleviate the impacts of this uncertainty on real-time operation, system operators (SO) schedule controllable generators in such a way that they can adjust their outputs when the actual conditions deviate from the operating plan. If the expected uncertainty is overestimated, the schedule may result in unnecessarily expensive dispatch. On the other hand, if the uncertainty is underestimated, the schedule might not be feasible in the real-time and may require expensive or undesirable corrective actions, such as starting up expensive generators or shedding load. A rigorous assessment of the required range of adjustments at various times over the optimization horizon is essential to obtain a cost-effective schedule.

Generating units are typically scheduled a day-ahead of the real time using a unit commitment (UC) program, which aims to commit the most cost-efficient combination of generation resources to serve the expected net load subject to operational constraints. The typical resolution of the UC problem is one hour; however, it can be reduced to intra-hour intervals to reduce the operating cost at the expense of computational time [1]. If the UC considers only a single net load forecast, this formulation is best described as a deterministic UC (DUC). This model accounts for uncertainty through the provision of some reserve generation capacity and the enforcement of ramping constraints within an operating hour [2], [3]. The amount of reserve capacity can be fixed during the course of the day [4], vary on a multi-hourly basis [5], or vary on the hourly basis [6], [7]. Because the DUC does not explicitly take into account more detailed information on the need for flexibility, such as the probability of a particular uncertainty realization, the schedule that it produces can be too conservative or insufficient during certain hours. As the penetration of renewable resources and, hence, the uncertainty on the net load increase [6], large deviations of the renewable generation make the DUC less and less attractive [8].

Stochastic UC (SUC) techniques, e.g., [9], [10], consider a set of net load forecasts, also called scenarios, and their probabilities to minimize the expected operating cost. As the number of scenarios in the SUC increases, so does the computation burden of the SUC formulation. This burden can be reduced by implementing a scenario reduction technique that lumps together similar scenarios [11], [12]. This approximation, however, reduces the accuracy of the uncertainty model and increases the operating cost [13], [14]. To facilitate practical implementation of the SUC in a large scale power system, decomposition approaches, based on the progressive hedging method [15] or Bender's decomposition [16], have been implemented. Since the SUC produces a single schedule for all scenarios, some optimality might be sacrificed for each individual scenario to minimize the expected operating cost over the entire set of scenarios. To reduce the impact of extreme scenarios with low probabilities, load shedding is allowed. In this case, the SUC may opt to shed load for an extreme scenario rather than commit more potentially expensive generators and sacrifice dispatch optimality over all scenarios. A trade-off between these decisions is sensitive to the value that an SO places on a unit of load shedding.

The interval UC (IUC) formulation [17] simplifies the representation of uncertainty used in the SUC by considering only a central forecast and upper and lower bounds on the net load,

Manuscript received September 20, 2013; revised January 31, 2014 and June 02, 2014; accepted June 13, 2014. This work was supported in part by the ARPA-E Green Electricity Network Integration (GENI) program under project DE-FOA-0000473 and in part by the State of Washington STARS program. The work of Y. Dvorkin was supported in part by the Clean Energy Institute's (University of Washington) Graduate Fellowship. Paper no. TPWRS-01212-2013.

The authors are with the Department of Electrical Engineering, University of Washington, Seattle, WA 98195-2500 USA (e-mail: dvorkin@uw.edu; hpandzic@uw.edu; maov@uw.edu; kirschen@uw.edu).

Color versions of one or more of the figures in this paper are available online at http://ieeexplore.ieee.org.

Digital Object Identifier 10.1109/TPWRS.2014.2331279

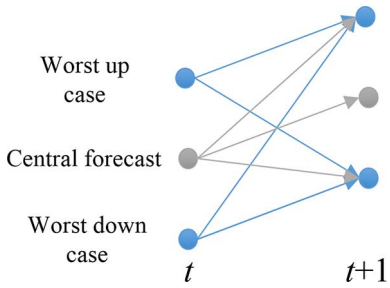

Fig. 1. Schematic representation of a given scenario set approximated for IUC.

as illustrated in Fig. 1. The objective function of the IUC minimizes the operating cost of the central forecast and enforces the feasibility of all inter-hour transitions within the bounds of uncertainty for adjacent operating hours. This approximation ensures that the IUC schedule is feasible for any scenario that remains within these bounds [18]. If the upper and lower bounds of the IUC envelope all scenarios used in the SUC, the solution of the IUC is proven to be feasible for all scenarios in the SUC [17]. However, in this case the IUC schedule is more expensive than the SUC schedule because it enforces inter-hour transitions with low probabilities at any cost [13].

In the robust UC (RUC) formulation [19], uncertainty is also represented by a central forecast and bounds. Instead of enforcing the feasibility of given transitions as in the IUC, the RUC performs a min-max optimization to protect the system against all realizations of uncertainty in a given range and to minimize the operating cost under the worst realization of uncertainty. This worst case simultaneously accounts for situations where there is little or no power produced by stochastic sources and for fast up or down ramps. While minimizing the cost for the worst case, the RUC solution is less cost effective for the central forecast. This problem is somewhat alleviated through the use of an uncertainty budget, which is a user-defined parameter that regulates the conservatism and cost efficiency of the RUC solution [19]. According to [19], the RUC is computationally tractable for large systems and its solution is cheaper than the solution produced by a DUC on the basis of the deterministic reserve criteria implemented by the ISO New England. In [20], a multi-stage robust formulation is applied to maximize social welfare under the joint worst-case wind power output and demand response scenario. The authors of [21] have proposed a unified stochastic and robust UC formulation that simultaneously enforces RUC and SUC constraints. The objective function of this formulation contains stochastic and robust terms, weighed using a heuristically determined parameter. In addition to this heuristics, this parameter is insensitive to monotonic nature of uncertainty in day-ahead planning and enforces the same ratio between conservatism and cost-efficiency for all hours of the optimization horizon.

The common thread of the DUC, SUC, IUC, and RUC models is that their objective functions seek to minimize the operating cost, while committing sufficient resources to accommodate a real-time materialization of uncertainty. However, these formulations differ in their representation of this uncertainty (even for the same sources of uncertainty) and, thus, result in different solutions.

This paper proposes a hybrid UC (HUC) formulation that combines the SUC and IUC formulations with the aim of achieving a solution that balances the operating cost and robustness. Unlike the unified formulation proposed in [21], which applies the SUC and RUC formulations simultaneously over the entire optimization horizon, the HUC implements the SUC and IUC formulations sequentially over this horizon. Over the first part of this horizon, the schedule is optimized using the cost-effective but computationally demanding SUC formulation. It then switches to the more robust but tractable IUC approach. As compared to [21], the proposed approach does not weigh two UC approaches heuristically. Instead, the switching time is optimized to balance the cost of unhedged uncertainty associated with the SUC schedule and the security premium embedded in the IUC schedule.

II. Hybrid Unit Commitment Formulation

In the following, we call *day-ahead cost* (DAC) the optimal value of the objective function of a particular UC formulation. The DAC of the SUC is the minimum expected operating cost over the set of scenarios. On the other hand, the DAC of the IUC is the cost of the schedule that minimizes the cost of meeting the central net load forecast while ensuring the feasibility of the pre-defined worst-case scenarios. These two formulations rely on different models of uncertainty and, consequently, may result in schedules with different capabilities to balance supply and demand in real-time. A more conservative uncertainty model results in a more conservative schedule and a greater DAC [22] due to a larger security cost [23]. The DAC calculated with any UC approach is usually different than the actual cost incurred on the day, because the realization of the stochastic sources of uncertainty may vary from its forecast. Dealing with unavoidable differences between the postulated and actual net load requires adjustments to the day-ahead schedule. These adjustments are known as corrective actions [24] and involve re-dispatching of generators committed, as well as starting up or shutting down other generators in response to these deviations. These corrective actions make the actual operating cost (AOC), incurred in the real-time, larger or smaller than the DAC. The difference between the AOC and the DAC is the *cost of corrective actions*, which can be positive or negative, depending on the error on the net load forecast. Each UC formulation thus results not only in a different security cost (because they account for uncertainty in different ways), but also different cost of corrective actions (because the resulting schedules require different real-time adjustments).

The HUC formulation aims to minimize the AOC by achieving the optimal balance between the day-ahead security cost and the expected cost of uncertainty associated with the day-ahead schedule.

A. Concept of Hybrid Unit Commitment

UC decisions are typically made in the day-ahead time frame based on forecasts of load and renewable generation for the following day. Since these forecasts are by nature uncertain, the SO must assume that the actual values will deviate from the anticipated values. These deviations start at the first operating hour of the following day and their expected magnitude increases during the course of the day, as Fig. 2 shows schematically.

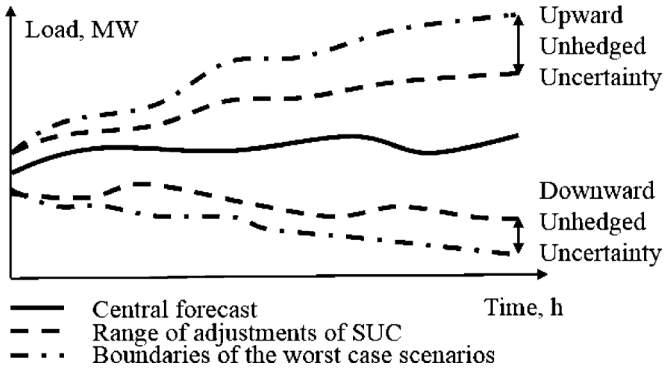

Fig. 2. Schematic representation of the unhedged uncertainty associated with the SUC solution.

In the process of minimizing the expected day-ahead operating cost over a set of scenarios, the SUC might decide that shedding some load or spilling some energy from renewable sources for some of the most extreme scenarios is cheaper than modifying the schedule in such a way that it can serve net load in all scenarios. In other words, and as illustrated in Fig. 2, the SUC solution carries a certain amount of unhedged uncertainty. Typically, this unhedged uncertainty increases over time. It can be quantified in terms of expected energy not served (EENS), sometimes referred to as load curtailment, and expected renewable energy spilled, also referred to as renewable curtailment. In turn, these quantities can be translated into a cost using the value of lost load (VoLL), also known as the cost of load curtailment, which represents the value that an SO puts on 1 MWh of energy not served, and the value of wind spillage (VoWS), also known as the cost of wind curtailment, which represents the marginal value of 1 MWh of wind spilled. The VoLL mainly depends on the type of the curtailed load, but can typically be determined based on customer surveys in a particular power system [25]. The VoWS is subject to jurisdictional variations and generally depends on tax credits and monetary incentives [26] or the loss of opportunity cost [27] of wind producers. Although the VoWS is currently used in many power systems, [28], its high value may result in an inefficient dispatch of conventional generators because it could lead to unnecessary cycling [26], [23].

On the other hand, the IUC formulation ensures that any scenario within a predefined range of uncertainty can be handled without having to resort to load shedding, regardless of the low probability associated with these scenarios. Therefore, the solution produced by the IUC has zero unhedged uncertainty. However, the improved operational reliability requires more committed capacity, resulting in a higher DAC than the SUC. The HUC strives to minimize the DAC by optimally balancing the security cost of the IUC against the cost of unhedged uncertainty of the SUC. It achieves this by taking advantage of the lower day-ahead cost of the SUC solution during the early hours of the optimization horizon, i.e., when the cost of the unhedged uncertainty is low, and then switching to an IUC solution, i.e., when this cost rises. As shown in Fig. 3, the SUC formulation is applied to the first $(t^{\mathrm{sw}}-1)$ hours of the optimization horizon. During these operating hours, the HUC formulation uses the same objective function, input scenarios, and constraints as the SUC. In this case, the HUC schedule obtained for hour $t \in [1, t^{\mathrm{sw}}-1]$ ought to acquire some of the features of

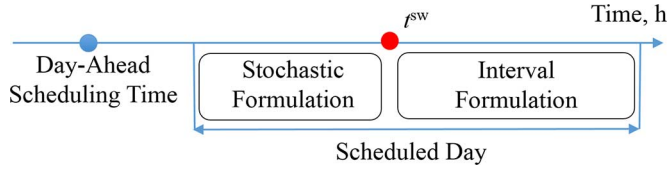

Fig. 3. Schematic representation of the hybrid unit commitment.

the SUC model, such as its relatively low expected cost and its real-time performance against actual realizations of uncertainty. The remaining operating hours, $t \in [t^{\mathrm{sw}}, T]$, are solved using the IUC formulation, i.e., during those hours the HUC mirrors the objective function, uncertainty model, and constraints of the IUC formulation. Consequently, this part of the HUC schedule aims to inherit the conservatism of the IUC model to be protected against the relatively large uncertainty levels at the end of the optimization horizon. Thus, the switching time t^{sw} should be chosen in such a way that the resulting HUC schedule combines the benefits of both the SUC and IUC models.

To ensure consistency between the SUC and IUC decisions, coupling constraints are enforced. These constraints account for inter-temporal limits on controllable generation, such as ramping limits and minimum up- and down-times. Switching to the IUC from the SUC at the end of the optimization horizon is also justified by a reduction in the forecast accuracy for individual scenarios as compared to the range of uncertainty. As reported in [29] and [30], the mean and standard deviation of the wind forecasting error for an individual scenario increases significantly for a prediction horizon of 6 h and more. The range of uncertainty in the IUC formulation can be adjusted in such a way that its bounds cover individual scenarios with a given level of confidence. As compared to the SUC, a larger range between bounds in the IUC does not require a larger number of scenarios and, therefore, does not increase the size of the optimization problem to be solved.

B. Mathematical Formulation

In the following equations, the indices i, s, b and t refer to the sets of controllable generators I, of scenarios S, of buses B, and of time intervals T, where $T^{\mathrm{SUC}} = [1, t^{\mathrm{sw}})$ and $T^{\mathrm{IUC}} = [t^{\mathrm{sw}}, \mathrm{card}(T)]$. Set of transmission lines is denoted by L.

The objective function of the HUC is

$$\begin{aligned}
&\min \sum_{t\in T}\sum_{i\in I}(\mathrm{SU}_{t,i} + \mathrm{SD}_{t,i}\cdot y_{t,i}) \\
&+ \sum_{i\in I}\left(\sum_{t\in T^{\mathrm{SUC}}}\pi_s \cdot \sum_{s\in S} F_i(p_{t,i,s}) + \sum_{t\in T^{\mathrm{IUC}}} F_i(p_{t,i,\mathrm{cf}})\right) \\
&+ \sum_{t\in T^{\mathrm{SUC}}}\sum_{b\in B}\sum_{s\in S}(\pi_s\cdot \mathrm{ENS}_{t,b,s}\cdot \mathrm{VoLL} + \pi_s\cdot \mathrm{WS}_{t,b,s}\cdot \mathrm{VoWS}_{t,b}) \\
&+ \sum_{t\in T^{\mathrm{IUC}}}\sum_{b\in B}(\mathrm{WS}_{t,b,\mathrm{cf}}\cdot \mathrm{VoWS}_{t,b}). \qquad (1)
\end{aligned}$$

The first term of this objective function accounts for the start-up cost, $\mathrm{SU}_{t,i}$, of generator i at hour t, as calculated in constraint (9), and the shutdown cost, $\mathrm{SD}_{t,i}$, of each generator i at hour t if the shutdown binary variable, $y_{t,i}$, is non-zero. The second term represents the expected dispatch cost and consists of two parts: the SUC day-ahead cost for the first T^{SUC} hours

and the IUC day-ahead cost for the remaining T^{IUC} hours. The SUC cost calculates the sum of the dispatch cost for each scenario weighed by the probability of this scenario. The IUC cost involves only the cost of the dispatch for central forecast (cf). Function $F_i(\cdot)$ accounts for the no-load cost and the variable cost of each generator using a piecewise-linear approximation of the convex cost curve. Since the cost curves are convex, no binary variables are needed to model this piecewise-linear approximation. Function $F_i(\cdot)$ divides the operation range of each generator in three segments with the constant incremental cost within each segment. The third term in (1) represents the cost of the energy not served (ENS) and wind spilled (WS), for each scenario over the period of time covered by the SUC formulation. These quantities are weighed by the probability of each scenario, π_s. Energy not served is monetized using the value of loss load, VoLL, while involuntary wind spillage is penalized at the value of wind spillage, VoWS. If there is no incentives for the wind producers or market rules to compensate the lost opportunity, the VoWS is set to \$0/kWh. The fourth term represents the cost of wind spilled over the period of time covered by the IUC formulation. Note that the IUC solution does not permit any load shedding, since this approach does not account for the likelihood of an individual scenario. The HUC optimization is subject to the following constraints:

1) Constraints on the Generation Commitment, Start-Up and Shutdown Binary Variables:

$$x_{t,i} - y_{t,i} = u_{t,i} - u_{t-1,i}, \quad \forall t \in T, i \in I \tag{2}$$

$$x_{t,i} + y_{t,i} \leq 1, \quad \forall t \in T, i \in I \tag{3}$$

$$u_{t,i} = g_{t,i}^{\mathrm{on/off}}, \quad \forall t \in \left[0, L_t^{\mathrm{up,min}} + L_t^{\mathrm{down,min}}\right], i \in I \tag{4}$$

$$\sum_{r=t-g_i^{\mathrm{up}}+1}^{t} x_{r,i} \leq u_{r,i}, \quad \forall t \in \left[L_t^{\mathrm{up,min}}, T\right], i \in I \tag{5}$$

$$\sum_{r=t-g_i^{\mathrm{down}}+1}^{t} y_{r,i} \leq 1 - u_{r,i}, \ \forall t \in \left[L_t^{\mathrm{down,min}}, T\right], i \in I \tag{6}$$

$$z_{t,i,j} \leq \sum_{r=suc_{i,j}^{\mathrm{lim}}}^{\min\left\{t-1, suc_{i,j+1}^{\mathrm{lim}}-1\right\}} y_{t-r,i}, \ \forall t \in T, i \in I, j \in J \tag{7}$$

$$\sum_{j \in J} z_{t,i,j} = x_{t,i}, \quad \forall t \in T, i \in I \tag{8}$$

$$\mathrm{SU}_{t,i} = \sum_{j \in J} \mathrm{suc}_{i,j} \cdot z_{t,i,j}, \quad \forall t \in T, i \in I. \tag{9}$$

Constraints (2) and (3) link the start-up $x_{t,i}$ and shutdown $y_{t,i}$ binary variables to the binary commitment variables $u_{t,i}$. Constraints (4)–(6) enforce the minimum up- and down-time requirements [31]. In these equations $g_i^{\mathrm{on/off}}$ denotes the on/off status of generator i at $t = 0$, g_i^{up} and g_i^{down} are the minimum up- and down-times of generator i, while $L_i^{\mathrm{up,min}}$ and $L_i^{\mathrm{down,min}}$ are the numbers of hours that generator i is required to stay on or off at the beginning of the optimization horizon. Only one of $L_i^{\mathrm{up,min}}$ and $L_i^{\mathrm{down,min}}$ can be greater than zero for each generator. Constraints (7)–(9) calculate the generator start-up cost $\mathrm{SU}_{t,i}$ [32]. Binary variable $z_{t,i,j}$ is equal to 1 if generator i is started at time t after being off for j hours, and 0 otherwise. Index j accounts for the number of hours that a generator has been off prior to its start-up. Parameter $\mathrm{suc}_{i,j}(\$)$ contains cost intervals for the step-wise cost curve, while parameter $\mathrm{suc}_{i,j}^{\mathrm{lim}}$ (h) provides time intervals for the start-up cost curve.

2) Constraints on the SUC Portion of the Optimization:

$$p_i^{\min} \cdot u_{t,i} \leq p_{t,i,s} \leq p_i^{\max} \cdot u_{t,i}, \ \forall t \in T^{\mathrm{SUC}}, i \in I, s \in S^{\mathrm{SUC}} \tag{10}$$

$$\sum_{i \in I_b} p_{t,i,s} + w_{t,b,s} - \mathrm{WS}_{t,b,s} - \sum_{\{m,b\} \in L | m > b} B_{m,b} \cdot (\delta_{t,b,s} - \delta_{t,m,s}) + \sum_{\{b,m\} \in L | m < b} B_{m,b} \cdot (\delta_{t,m,s} - \delta_{t,b,s}) = d_{t,b}, \ \forall t \in T^{\mathrm{SUC}}, k \in S^{\mathrm{SUC}}, b \in B \tag{11}$$

$$p_{t,i,s} - p_{t-1,i,s} \leq RU_i, \quad \forall t \in T^{\mathrm{SUC}}, i \in I, s \in S^{\mathrm{SUC}} \tag{12}$$

$$p_{t-1,i,s} - p_{t,i,s} \leq RD_i, \quad \forall t \in T^{\mathrm{SUC}}, i \in I, s \in S^{\mathrm{SUC}} \tag{13}$$

$$-f_{\{b,m\}}^{\max} \leq B_{b,m} \cdot (\delta_{t,b,s} - \delta_{t,m,s}) \leq f_{\{b,m\}}^{\max} \quad \forall t \in T^{\mathrm{SUC}}, \{b,m\} \in L, s \in S^{\mathrm{SUC}} \tag{14}$$

$$\mathrm{ENS}_{t,b,s} \leq d_{t,b,s}, \quad \forall t \in T^{\mathrm{SUC}}, s \in S^{\mathrm{SUC}}, b \in B \tag{15}$$

$$\mathrm{WS}_{t,b,s} \leq w_{t,b,s}, \quad \forall t \in T^{\mathrm{SUC}}, s \in S^{\mathrm{SUC}}, b \in B. \tag{16}$$

Constraints (10) enforce the minimum, $p^{\min}$, and maximum, $p^{\max}$, limits on the power output of the controllable generators in all stochastic scenarios $s \in S^{\mathrm{SUC}}$ and over time periods $t \in T^{\mathrm{SUC}}$. Constraints (11) are the power balance equations. The term $\sum_{i \in I_b} p_{t,i,s}$ represents the sum of outputs of all controllable generators connected to bus b, i.e., $I_b \subseteq I$, $w_{t,b,s}$ is the wind energy available at bus b, and $\mathrm{WS}_{t,b,s}$ is the wind energy spilled. The last two terms on the left-hand side are the power flows from and into bus b, where B_{bm} is the admittance of the line connecting buses b and m, and $\delta_{t,b,s}$ is the voltage angle. The net power inflow at every bus b has to be equal to the bus load $d_{t,b,s}$ minus the energy not served $\mathrm{ENS}_{t,b,s}$. Constraints (12)–(13) enforce the ramp up and ramp down rates of the controllable generators. Constraints (14) enforce the maximum line flow limits, $f^{\max}$, via a linear dc power flow model. The dc power flow formulation approximates the ac model, but represents the transmission constraints with sufficient accuracy for the day-ahead planning and active power analysis [33] and has been used in the previous UC studies [13], [19]. A new approach to reduce the computation burden of the dc power flow formulation using umbrella constraints has been proposed in [34]. References [33] and [35] compare the advantages and drawbacks of the dc and ac power flow models. Constraints (15) and (16) limit the load shedding and wind spillage at each bus to the forecast demand and wind production at these buses under the different scenarios.

3) Constraints on the IUC Portion of the Optimization:

$$p_i^{\min} \cdot u_{t,i} \leq p_{t,i,k} \leq p_i^{\max} \cdot u_{t,i}, \ \forall t \in T^{\mathrm{IUC}}, k \in S^{\mathrm{IUC}}, i \in I \tag{17}$$

$$\sum_{i \in I_b} p_{t,i,k} + w_{t,b,k} - WS_{t,b,k} - \sum_{\{b,m\} \in L | m > b} B_{b,m} \cdot (\delta_{t,b,k} - \delta_{t,m,k}) + \sum_{\{b,m\} \in L | m < b} B_{m,b} \cdot (\delta_{t,m,k} - \delta_{t,b,k}) = d_{t,b}, \quad \forall t \in T^{\mathrm{IUC}}, k \in S^{\mathrm{IUC}}, b \in B \tag{18}$$

$$p_{t,i,k} - p_{t-1,i,k} \leq RU_i, \quad \forall t \in T^{\mathrm{IUC}}, k \in S^{\mathrm{IUC}}, i \in I \tag{19}$$

$$p_{t-1,i,k} - p_{t,i,k} \leq RD_i, \quad \forall t \in T^{\mathrm{IUC}}, k \in S^{\mathrm{IUC}}, i \in I \tag{20}$$

$$-f^{\max}_{\{b,m\}} \leq B_{b,m} \cdot (\delta_{t,b,k} - \delta_{t,m,k}) \leq f^{\max}_{\{b,m\}}, \quad \forall t \in T^{\mathrm{IUC}}, \{b,m\} \in L, k \in S^{\mathrm{IUC}} \tag{21}$$

$$WS_{t,b,k} \leq w_{t,b,k}, \quad \forall t \in T^{\mathrm{IUC}}, k \in S^{\mathrm{IUC}}, b \in B \tag{22}$$

$$p_{t,i,\mathrm{ub}} - p_{t-1,i,\mathrm{cf}} \leq RU_i, \quad \forall t \in T^{\mathrm{IUC}}, i \in I \tag{23}$$

$$p_{t-1,i,\mathrm{cf}} - p_{t,i,\mathrm{lb}} \leq RD_i, \quad \forall t \in T^{\mathrm{IUC}}, i \in I \tag{24}$$

$$p_{t,i,\mathrm{ub}} - p_{t-1,i,\mathrm{lb}} \leq RU_i, \quad \forall t \in T^{\mathrm{IUC}}, i \in I \tag{25}$$

$$p_{t-1,i,\mathrm{ub}} - p_{t,i,\mathrm{lb}} \leq RD_i, \quad \forall t \in T^{\mathrm{IUC}}, i \in I. \tag{26}$$

Constraints (17)–(22) are the IUC equivalents of the SUC constraints (10)–(16). The only difference is that the SUC formulation considers stochastic scenarios, while the IUC formulation considers three scenarios: central forecast (cf), lower bound (lb) and upper bound (ub). These scenarios constitute set S^{IUC}. Constraints (20) and (23)–(26) enforce feasibility for all seven inter-hour transitions as illustrated in Fig. 1 and as explained in the original IUC model in [17]. However, constraints (23) and (24) can be removed from the model, since they hold automatically because of constraints (25) and (26). Note that since the IUC formulation does not allow any load shedding, its central forecast and bounds must be served at any cost, which may result in infeasibility. To avoid this problem, slack variables can be introduced in the power balance and power flow constraints. These slack variables must be penalized in the objective function by a sufficiently large price.

4) Coupling Constraints Between SUC and IUC:

$$p_{t^{\mathrm{sw}},i,k} - p_{t^{\mathrm{sw}}-1,i,s} \leq RU_i, \ \forall i \in I, \forall s \in S^{\mathrm{SUC}}, \forall k \in S^{\mathrm{IUC}} \tag{27}$$

$$p_{t^{\mathrm{sw}}-1,i,s} - p_{t^{\mathrm{sw}},i,k} \leq RD_i, \ \forall i \in I, \forall s \in S^{\mathrm{SUC}}, \forall k \in S^{\mathrm{IUC}}. \tag{28}$$

Constraints (27)–(28) ensure that the difference between dispatch decisions for each scenario s at hour $(t^{\mathrm{sw}} - 1)$ made by the SUC and for each scenario k at hour t^{sw} made by the IUC meet the limitations on the ramp rates of committed generators. If these constraints are enforced, the resulting schedule will be able to ramp between the SUC and IUC parts of the schedule.

The operating cost of the HUC (C^{HUC}) is a function of the switching time t^{sw}. If the switching time is zero the HUC is equivalent to the IUC and $C^{\mathrm{HUC}} = C^{\mathrm{IUC}}$. If the switching takes place at early periods, the cost of the HUC will be close to the cost of the IUC because the SUC formulation will be applied only for a few time periods and the resulting schedule will be obtained based mostly on the IUC. As the switching time increases, the DAC decreases at the expense of exposing the system to low probability events. If switching occurs later, ramping and inter-temporal generator constraints of the SUC solution limit a number of generators available to improve the robustness of the schedule. Thus, the IUC may not be as cost-effective as it would have been if applied to the whole optimization horizon. Finally, if no switching takes place in the solution process, the HUC is equivalent to the SUC and $C^{\mathrm{HUC}} = C^{\mathrm{SUC}}$.

Hedging the system against all possible realizations of uncertainty can be achieved with an early t^{sw}. However, this would result in a high operating cost. The HUC therefore needs to strike a balance between its running cost (RC) and the economic savings achieved by allowing some unhedged uncertainty. The running cost accounts for the cost of commitment decisions and dispatch:

$$\mathrm{RC}(t^{\mathrm{sw}}) = \sum_{t \in T} \sum_{i \in I} (\mathrm{SU}_{t,i} + \mathrm{SD}_{t,i} \cdot y_{t,i}) + \sum_{i \in I} \left(\sum_{t \in T^{\mathrm{SUC}}} \sum_{s \in S^{\mathrm{SUC}}} \pi_s \cdot F_i(p_{t,i,s}) + \sum_{t \in T^{\mathrm{IUC}}} F_i(p_{t,i,\mathrm{cf}}) \right). \tag{29}$$

Therefore, the running cost increases as the switching time decreases since more hours are solved using the conservative IUC formulation. As the switching increases, there are more periods during which the SUC dominates the solution, increasing the allowed unhedged uncertainty. The Cost of unhedged Uncertainty, CoU, is then given by

$$CoU(t^{\mathrm{sw}}) = \sum_{t \in T^{\mathrm{SUC}}} \sum_{b \in B} \sum_{s \in S^{\mathrm{SUC}}} (\pi_s \cdot ENS_{t,b,s} \cdot VoLL + \pi_s \cdot WS_{t,b,s} \cdot VoWS_{t,b}) + \sum_{t \in T^{IUC}} \sum_{b \in B} (WS_{t,b,\mathrm{cf}} \cdot VoWS_{t,b}) \tag{30}$$

where $\mathrm{ENS}_{s,t}$ and $\mathrm{WS}_{s,t}$ are the energy not served and the wind spilled at time t for scenario s. The cost in (30) accounts for the unhedged uncertainty predicted on the day ahead. Although an actual realization may exceed the most extreme scenario considered in the day-ahead planning, such an event cannot be precisely predicted in the day ahead and, therefore, cannot be considered in the decision-making process. On the other hand, this realization can be handled by real-time adjustments.

Since the value of the optimal switching time depends on the relative proportion between the running cost and the cost of unhedged uncertainty, it can be affected by variations on the right-hand-side of (29) and (30). For example, if the generation fleet has limited flexibility, then the transition between the proposed schedules might be impossible due to inter-temporal constraints on generators. Also, high start-up and fuel costs can make switching prohibitively expensive. If the range of scenarios in the SUC is relatively narrow, the unhedged uncertainty might be insufficient to switch to a more expensive IUC solution. Similarly, if the $VoLL$ or $VoWS$ are relatively low, this may result in no switching, because providing the additional robustness of the IUC would not be economically justified. Therefore, accurately estimating the $VoLL$ and $VoWS$, as well as improving forecasting accuracy, an SO can change the switching time. The next subsection describes two approaches to optimize t^{sw}.

C. Optimal Switching Time

As explained in Section II-B, the switching time minimizes the objective function of the HUC via balancing its running cost and cost of unhedged uncertainty. The operating cost of HUC, C^{HUC}, is a function of the switching time. As the switching time increases, the running cost decreases, as shown in (29), while the cost of unhedged uncertainty increases, as shown in (30). Therefore, the operating cost of the HUC, C^{HUC}, which sums the running cost and the cost of unhedged uncertainty, is guaranteed to have a minimum. Since the commitment or de-commitment of a generator changes the value of the cost of

unhedged uncertainty and the running cost abruptly, this function can have local minima, which makes it almost unimodal.[1] Therefore, traditional derivative-based methods to calculate its minimum are not applicable due to the risk of being trapped in a local minimum. The domain of the switching time is limited to a finite number of integer solutions over the interval $[1, \mathrm{card}(T)]$. Therefore, the minimum of $C^{\mathrm{HUC}}(t^{\mathrm{sw}})$ can be obtained by solving the HUC formulation at most $\mathrm{card}(T)$ times. This can be done using a parallel implementation or a single processor implementation, as discussed below.

1) Parallel Computing Implementation: Parallel computing makes it possible to carry out multiple simulations at the same time. In this implementation, each parallel simulation solves the HUC problem for a particular value of the switching time and produces its cost, $C^{\mathrm{HUC}}(t^{\mathrm{sw}})$. Therefore, the HUC formulation is solved $\mathrm{card}(T)$ times. When all parallel simulations are completed, the optimal switching time is determined as the minimum of $C^{\mathrm{HUC}}(t^{\mathrm{sw}})$. The computation time τ of the parallel implementation is then determined as the maximum computation time of all parallel simulations, i.e., $\tau = \max[\tau^{t^{\mathrm{sw}}=1}, \tau^{t^{\mathrm{sw}}=2}, \ldots, \tau^{t^{\mathrm{sw}}=\mathrm{card}(T)}]$.

2) Single Processor Implementation: Since a single processor is not able to carry out multiple simulations at the same time, the single processor implementation solves the HUC problems in series, i.e., this implementation requires solving the HUC formulation $\mathrm{card}(T)$ times consecutively. To reduce the required number of iterations, a search method can be used. A three-point grid search algorithm, a derivative-free search method, has been shown to converge and estimate the optimum of the almost unimodal functions precisely [37]. As proven in [37], this method has linear convergence and has already been applied in power system applications dealing with uncertainty [22]. This algorithm operates as follows. First, an interval $[T^{\mathrm{LB}}, T^{\mathrm{UB}}]$ containing t^{sw} is chosen. Second, three equally spaced points within the search interval, $[t^{\mathrm{sw1}}, t^{\mathrm{sw2}}, t^{\mathrm{sw3}}]$, are chosen and the HUC, as formulated in (1)–(26), is solved for each of them. Third, two neighbors (possibly including one of the bounds of the interval) of the points among these three that give lowest values of C^{HUC} are chosen as the bounds of the next search interval. This procedure is repeated until the optimal t^{sw} is found with enough accuracy. Since the domain of the switching time is finite, the optimal switching time can be found in a finite number of iterations. The search range of the switching time reduces by $(1/4)^n$ after $n > 1$ iterations [37], if the cost function, C^{HUC}, is strictly unimodal. In practice, the cost function is almost unimodal and, therefore, the convergence of the three-point grid search algorithm is less efficient in this case. However, the algorithm has also been proven to "*find a reasonable solution for an almost unimodal function*" [37]. Although the three-point grid search algorithm reduces the number of solution candidates, its computation time consists of the sum of computation times of all iterations. Therefore, the computation time of the single processor implementation would be larger compared to the computation time of the parallel computing implementation. Additionally, the parallel computing implementation is immune to assumptions regarding the unimodality of the cost function.

[1]A function f is almost (noisy) unimodal in $[a, b]$, if and only if for some $x \in [a, b] f' < 0$ almost everywhere on $[a, x]$ and $f' > 0$ almost everywhere on $[x, b]$ [36]. Examples of almost unimodal functions can be found in [36] and [37].

TABLE I
SUMMARY OF DIFFERENT UC FORMULATIONS

Number of	DUC	SUC	IUC	HUC
binary variables	8,448	8,448	8,448	8,448
continuous variables	15,148	73,900	35,308	35,308–73,900
constraints	22,019	128,291	63,299	63,939–128,931

III. CASE STUDY

A. Data and Test System

The proposed HUC, as well as the DUC, SUC, and IUC formulations have been tested on a modified version of the 24-bus IEEE Reliability Test System. Details of this system can be found in [38]. The cost curves of the generating units in this system are approximated by three-segment piece-wise linear functions with equally spaced elbow points. Generators U12 and U20 can be synchronized or shutdown within a single operating hour. The wind and load data are based on ERCOT data [39]. The wind penetration is assumed to provide 10% of electricity consumed daily system-wide. A set of 1000 wind scenarios were generated as described in [40]. A forward selection scenario reduction technique reduced this set to 10 scenarios used by the SUC [13], [41]. The $5-$ and $95-$percentiles of the original set were used to define the lower and upper bounds for the IUC. These bounds envelope all scenarios in the SUC. In the reference case $VoLL = \$5$/kWh for all operating hours and the $VoWS$ is calculated based on the lost opportunity of wind producers for each operating hour. This lost opportunity cost of wind producers is calculated as the difference between two cases: when wind curtailment is not enforced and when wind curtailment is enforced, as explained in [27].

The HUC formulation is as described in (1)–(28) and the switching time is optimized as described in Section II-C. The SUC formulation includes constraints (2)–(16) and the IUC formulation includes constraints (2)–(9) and (17)–(26). The DUC formulation is identical to the IUC but without bounds and without constraints (23)–(26). Table I compares the DUC, SUC, IUC, and HUC formulations in terms of the number of variables and constraints. All formulations have the same number of binary variables: $x_{t,i}, y_{t,i}, u_{t,i} - 768$ each, $z_{t,i,j} - 6\ 144$. The number of continuous variables and constraints differ for each formulation: the DUC and the SUC have respectively the smallest and the largest number of continuous variables and constraints. Since the optimal switching hour is unknown until the HUC is solved, the number of continuous variables is characterized by a range of the SUC and IUC formulations, as shown in Table I. The number of constraints in the HUC is also characterized by this range plus the number of coupling constraints (27) and (28).

Simulations for this case study have been performed on a PC with an Intel® Core i7 2.80-GHz processor and 4 GB of RAM under the 64-bit Windows® 7 operating system. The CPLEX 12.1 optimization engine and the GAMS 24.0.2 environment have been used to implement all UC formulations. The minimum relative MIP gap has been set to 10^{-3}.

TABLE II
DAY-AHEAD COSTS FOR DIFFERENT UC APPROACHES (IN 10^3, \$)

	VoLL=\$1/kWh			VoLL=\$5/kWh			VoLL=\$10/kWh		
	DAC	SC	CoU	DAC	SC	CoU	DAC	SC	CoU
DUC	897	29	2	897	29	2	897	29	2
SUC	899	31	13	908	40	9	912	44	7
IUC	1022	154	4	1022	154	4	1022	154	4
HUC	908	41	8.3	958	99	34	973	105	67

B. Day-Ahead Cost of the DUC, SUC, and IUC

Table II shows the day-ahead cost (DAC), security cost (SC), and the cost of unhedged uncertainty (CoU) for the DUC, SUC, and IUC formulations for different $VoLL$s. The security cost is calculated as the difference between the day-ahead operating cost of a particular UC approach and the day-ahead cost of the DUC formulation without reserve requirements. Since the DUC accounts for a single central forecast scenario, this formulation results in the least expensive day-ahead and security costs for any $VoLL$. The SUC formulation models uncertainty via a set of scenarios and, therefore, it results in a larger day-ahead and security costs. Since the DUC does not tolerate any load shedding, its cost of unhedged uncertainty is incurred by the cost of wind spillage. The IUC results in the most conservative day-ahead schedule, which results in the largest day-ahead and security cost among all UC formulations. Since the IUC does not enable load shedding, its cost of unhedged uncertainty includes the cost of wind spillage only and, thus, it is less than for the SUC.

C. Day-Ahead Costs of the HUC

Table II presents day-ahead results of the HUC for different $VoLLs$. Fig. 4 shows how the day-ahead cost (DAC), the running cost (RC), and the cost of the unhedged uncertainty (CoU) of the HUC vary as a function of t^{sw} and compares it to the day-ahead cost of the SUC and IUC for $VoLL = \$5$/kWh. The cost of unhedged uncertainty of the HUC increases as the switching time increases because more operating hours are solved using the SUC formulation and thus more unhedged uncertainty is allowed in the resulting schedule. The running cost is also a function of the switching time, but it is not monotonic in [1] and [24] as the cost of the unhedged uncertainty. As illustrated in Fig. 4, the day-ahead cost decreases almost everywhere over the interval [1], [16] and increases over the interval [16], [24]. Note that this function increases from hour 6 to hour 7, which makes it almost unimodal in [1] and [24].

If the switching occurs early in the optimization horizon, the solution would be conservative, so an increment in the switching time causes a reduction in the objective function. However, a later switching requires the enforcement of the IUC boundaries subject to commitment decisions made previously on the day. This constrains the cycling of base load generators and requires committing expensive flexible generation, which cause a slight increase in the running cost at the end of the optimization horizon. Thus, both the cost of unhedged uncertainty and the running cost (and thus the day-ahead cost of the HUC) increase at the end of the optimization horizon, which makes late switching less cost-efficient. Fig. 5 illustrates the difference for the optimal generation pool committed by the HUC formulation with different $VoLLs$. As the VoLL increases, the

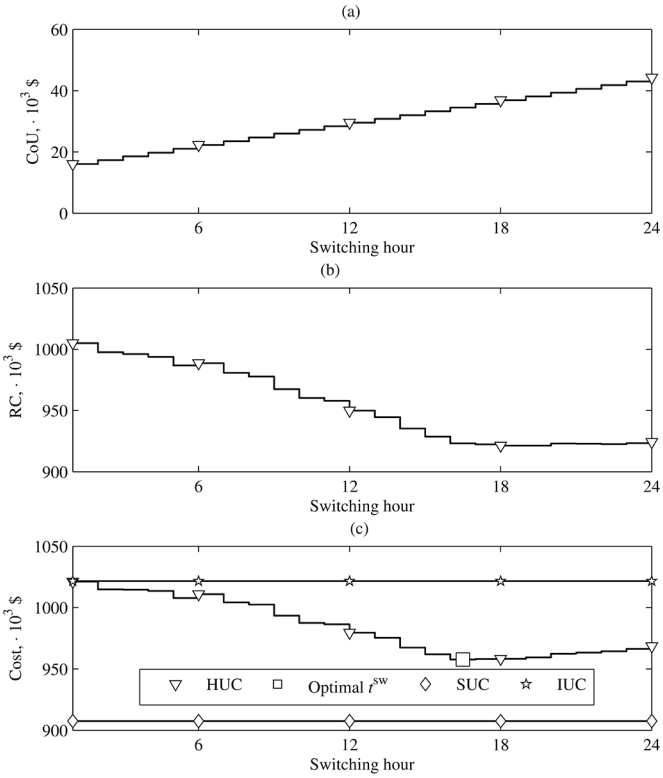

Fig. 4. (a) Cost of unhedged uncertainty. (b) Running cost of the HUC formulation. (c) Comparison of the total day-ahead costs of the IUC, SUC, and HUC formulations. The optimal switching time is highlighted with a square.

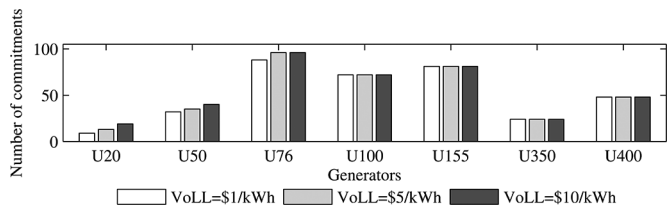

Fig. 5. Comparison of the cumulative number of commitments by the HUC throughout the optimization horizon for different VoLLs.

HUC formulation tends to commit more generators of the types U20, U50, and U76, while the number of commitment of other generators, which are less flexible, remains unchanged.

D. Optimizing the Switching Time

The switching time optimization has been performed as described in Section II-C for the parallel computing implementation and the single processor implementation. The domain of the switching time in the reference case is integer numbers in [1] and [24], $VoLL = \$5$/kWh, and the optimal switching hour is 16. Fig. 6 shows the computation time of the HUC formulation for different switching times and its trend approximated with a polynomial function. As the switching time increases so does the computation time due to an increased number of constraints and continuous variables, as shown in Table I.

1) Parallel Computing Implementation: In the parallel implementation, the HUC formulation is solved for all 24 values of the switching time simultaneously. The overall time of the parallel implementation is equal to the longest computation time of

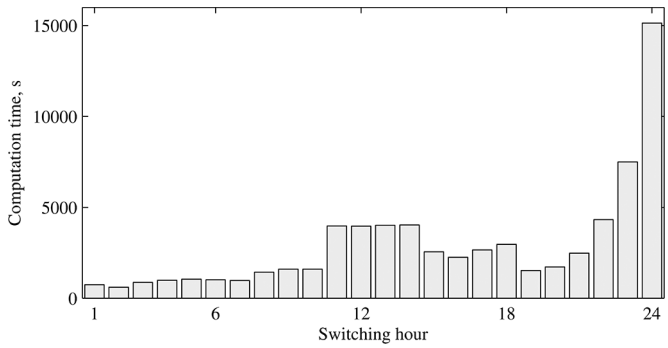

Fig. 6. Computation time of the HUC formulation with different switching times.

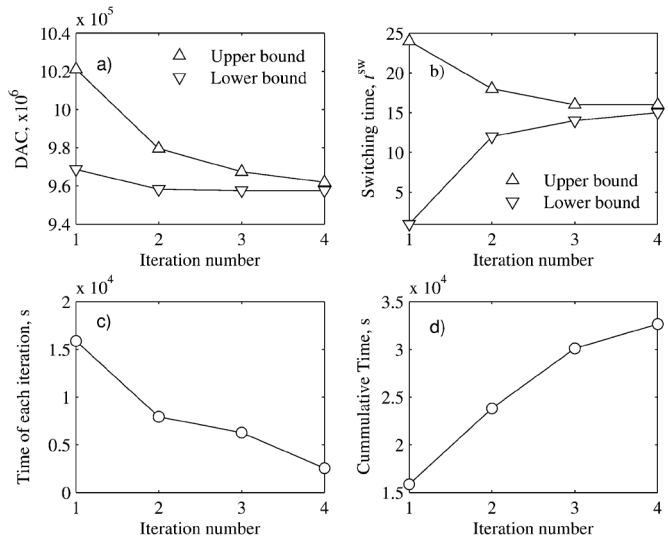

Fig. 7. Convergence of the HUC formulation in the single processor implementation: (a) the day-ahead cost (DAC) as the function of the switching, (b) the lower and upper bounds as the function of the switching time, (c) the CPU time of each iteration, and (d) the cumulative CPU at kth iteration.

all parallel simulations as explained in Section II-C. In the reference case $\tau = 15,135$ s (4 h:12 m:15 s), which is also equal to the computation time of the SUC formulation. The computation time of the HUC formulation is longer than the computation time of the IUC formulation—332 s (6 m:32 s).

2) Single Processor Implementation: In the single processor implementation case, four iterations of the three-point grid search method are required to obtain the optimal switching time. The range between the upper and lower bounds of the day-ahead cost decreases at each iteration [Fig. 7(a)] and so does the range between the upper and lower bounds of the switching time [Fig. 7(b)]. Fig. 7(c) shows the computation time for each iteration, which are added together in Fig. 7(d). The first iteration is the longest, because it involves solving the SUC formulation for the whole optimization horizon and thus involves more continuous variables and constraints than any other iteration. As the number of iterations increases, the duration of each iteration decreases because the upper bound of the switching time reduces and more operating hours are solved by the IUC. The overall computation time for the reference case in the single processor implementation is 32 647 s (9h:4m:7s).

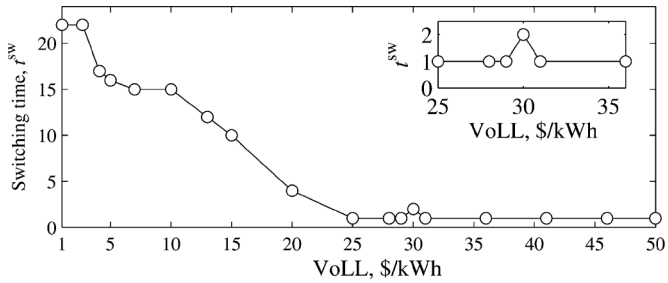

Fig. 8. Optimal switching time as a function of the VoLL.

3) Impact of the VOLL: Since the switching time determines a number of hours solved by the SUC and the IUC, it depends on the $VoLL$ chosen. Fig. 8 shows how this switching time varies as a function of the $VoLL$. Scheduling the generating fleet with a higher VoLL results in an earlier switching time and therefore more hours are solved by the IUC, which makes the schedule more robust and thus avoids having to resort to load curtailment. As the $VoLL$ changes, the commitment status of generators, the cost of uncertainty and the security cost may change as well. These changes are discrete due to the indivisible nature of binary commitment decisions on generating units, as explained in [22]. Hence, there might also be some fluctuations in the switching time for an incremental change in the $VoLL$. The inset of Fig. 8 shows that the switching time has a local extremum for $VoLL = \$30$/kWh

4) Impact of the Domain of the Switching Time: As Fig. 6 illustrates, if the switching occurs at the end of the optimization horizon, a longer computation time is requried because of the larger number of hours solved using SUC formulation. If the initial domain of the switching time is reduced in a way that avoids these computationally intensive calculations, the HUC can be solved faster. This, however, may result in a sub-optimal solution, because the truncated operating hours may contain the optimal switching time, especially, if the $VoLL$ is relatively high or low, as illustrated in Fig. 8. To demonstrate the computing performance of the HUC formulation with a reduced interval of possible switching times, the interval of switching times is limited to the hours between the beginning of the morning ramp and the peak net load. This rule-of-thumb was validated on a set of representative net load profiles for six days. This set includes four representative days for each calendar season and two days with the maximum and minimum daily net load.

In this case study, reducing a switching time by one hour will eliminate 1608 continuous variables and 2708 constraints from the HUC formulation. If the domain of the switching time is reduced to the interval between hour 8 (beginning of the morning ramp) and hour 19 (the interval of switching times), the parallel computing implementation is solved in 4027 s (1 h:7 m:7 s) and the single processor implementation is solved in three iterations, which require 13 203 s (3 h:40 m:3 s). Therefore, both implementations are solved faster than the SUC formulation.

5) Impact of the Switching Time on Committed Capacity: Fig. 9 compares the hourly committed capacity (CC) for the day-ahead schedules obtained with the SUC, IUC, and HUC with the optimal switching time for $VoLL = \$5$/kWh. Until the switching at hour 16, the HUC has a pattern similar to the committed capacity of the SUC. After the switching occurs, the

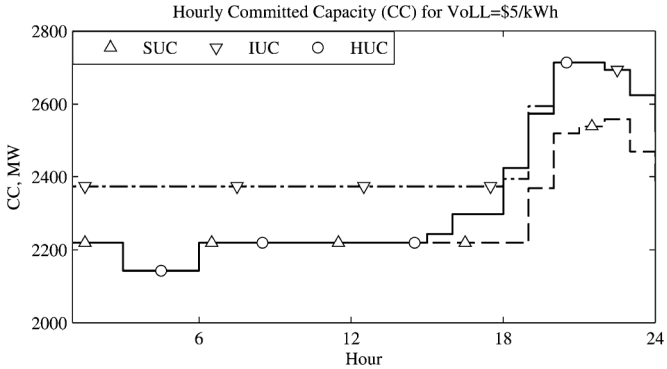

Fig. 9. Comparison of the hourly committed capacity for the day-ahead schedules of IUC (dash-dot), SUC (dash-dash), and HUC (solid) formulations.

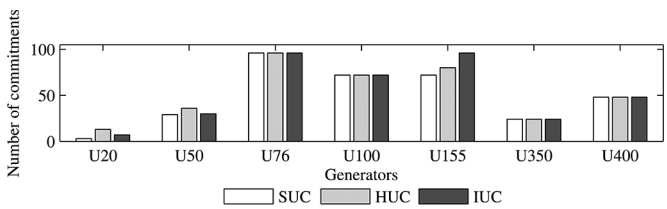

Fig. 10. Comparison of the cumulative number of commitments by different UC approaches throughout the optimization horizon.

HUC reaches the same committed capacity as the IUC approach at hour 19. In between, the HUC achieves the robustness of the IUC using a smaller amount of committed capacity but with more flexible (and therefore more expensive) units than the IUC. During the remainder of the optimization horizon, the hourly committed capacity of the HUC schedule repeats the trend of the hourly committed capacity of the IUC schedule. Fig. 10 shows the difference between the committed generation pool under different UC approaches. The same number of inflexible and relative cheap generators, such as U100, U350, and U400, are committed using any of the approaches. This figure also shows that the HUC has the largest number of commitments of flexible generators U20 and U50 so it can enforce its robustness after the switching occurs. Since the IUC needs to provide robustness during the course of the whole optimization horizon, it commits the largest number of inflexible generators U155.

E. Results of Monte Carlo Simulations

The statistical behavior of the schedules obtained with each of the UC approaches was tested using Monte Carlo simulations. At each trial of the Monte Carlo simulation the day-ahead schedule produced by each method is dispatched to meet the actual net load. Real-time commitments of additional generators are allowed if the day-ahead inter-temporal constraints on generators are not violated. At each Monte Carlo trial the corresponding value of the actual operating cost (AOC) is calculated. This AOC includes the generation dispatch and start-up costs based on the day-ahead schedule as well as the cost of additional commitments required in the real time and penalties for wind spillage and load shedding. The number of Monte Carlo trials required is set at $\min[1000, N_{\mathrm{MC}}]$, where N_{MC} is the number of Monte Carlo trials required to ensure with a 95% confidence level that the estimate of the AOC has an error of less than 1%

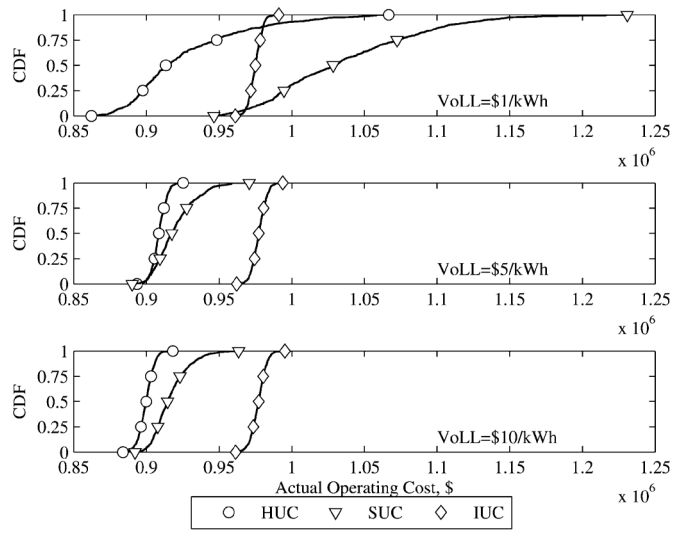

Fig. 11. Cumulative distribution function (CDF) of the actual operating cost AOC obtained with Monte Carlo simulations for different $VoLLs$.

TABLE III
STATISTICS OF MONTE CARLO SIMULATIONS FOR DIFFERENT $VoLL$ (COSTS ARE IN 10^3, \$)

VoLL	Variable	HUC	SUC	IUC
\$1/kWh	$C^{\min}$	863.1	939.4	961.2
	$E(C)$	926.9	1037.0	975.0
	$C^{\max}$	1079.5	1216.7	991.3
	$E(\Delta)$	18.9	138	-47
	$\sigma(C)$	42	53	0.45
	ENS, MWh	36.1	62.3	0
	WS, MWh	33.4	26.1	29.3
\$5/kWh	$C^{\min}$	892.7	889.5	961.3
	$E(C)$	908.7	919.6	977.4
	$C^{\max}$	922.8	969.6	995.1
	$E(\Delta)$	-49.3	11.6	-44.6
	$\sigma(C)$	0.47	1.4	0.46
	ENS, MWh	0.019	0.34	0
	WS, MWh	21.7	18.5	24.3
\$10/kWh	$C^{\min}$	883.2	891.5	960.8
	$E(C)$	899.7	916.7	977.1
	$C^{\max}$	916.6	964.9	993.6
	$E(\Delta)$	-73.3	2.6	-44.9
	$\sigma(C)$	0.50	1.2	0.47
	ENS, MWh	0.006	0.021	0
	WS, MWh	22.8	14.3	24.6

[42]. A normal distribution and a skew-Laplace distribution are assumed for the load forecast errors [43] and the wind power forecast errors [44], respectively.

Fig. 11 shows the cumulative probability distributions (CDFs) of the AOC, as calculated using Monte Carlo simulations. Table III gives the expected AOC (C), the maximum AOC $C^{\max}$, the minimum AOC $C^{\min}$, the expected cost of the corrective actions $E(\Delta)$, the standard deviation of the AOC distribution $\sigma(C)$, and the expected values of ENS and WS.

These Monte Carlo simulations demonstrate that the HUC schedule results in the lowest AOC for any $VoLL$, as compared to the SUC and IUC schedules. For $VoLL = \$1/\mathrm{kWh}$,

the SUC and HUC result in a positive expected cost of corrective actions, since these schedules were not optimized to accommodate large deviations from the forecast and underestimate the influence of uncertainty. The cost of corrective dispatch for the HUC schedule is less expensive than for the SUC schedule, which demonstrates that the HUC formulation models uncertainty more accurately than the SUC. The IUC results in an unnecessarily robust schedule as compared to the HUC and SUC formulations and has a negative expected cost of corrective dispatch, which indicates that the IUC formulation is likely to overestimate uncertainty. As $VoLL$ increases, the schedules obtained with all UC formulations become more robust and its cost of corrective dispatch decreases. If $VoLL = \$5$/kWh or $VoLL = \$10$/kWh, the SUC does not schedule sufficient resources to meet the deviations and results in a positive expected cost of corrective actions. On the other hand, the HUC schedule for $VoLL = \$5$/kWh and $VoLL = \$10$/kWh results in a negative expected cost of corrective actions. Although the HUC formulation overestimates uncertainty, the absolute value of the expected cost of corrective dispatch in this case is lower than for the IUC formulation. The low standard deviation of the AOC distribution in case of the HUC demonstrates its adaptability to extreme cases. In particular, for $VoLL = \$5$/kWh and $VoLL = \$10$/kWh the upper tail of the CDF of the HUC is shorter than the tails for the IUC and SUC (lower $C^{\max}$). Large $VoLLs$ amplify this effect because they justify an increase in the robustness of the schedule to deal with extreme cases. Because the IUC schedule is insensitive to the $VoLL$, its standard deviation remains nearly constant and it achieves the lowest ENS for all cases. On the other hand as the $VoLL$ increases, the ENS of the HUC decreases, because more periods are solved with the IUC constraints. While the SUC is also sensitive to the $VoLL$, its schedules do not balance the security costs against the ENS costs as well as the HUC. Unlike load shedding, the expected wind spillage remains approximately the same for all UC formulations because the penalty for spillage is significantly smaller than $VoLL$.

Table IV compares UC formulations under different wind penetration levels for $VoLL = \$5$/kWh. The HUC results in the lowest expected cost for all wind penetration levels. The HUC formulation is attractive to the SO, because it achieves savings from 1.2% to 3.9% for 10% and 30% wind penetration, respectively, as compared to the SUC. Furthermore, the HUC results in lower wind spillage than any other UC formulation for 20% and 30% wind penetration levels and also results in less load shedding than the SUC. The IUC formulation consistently overestimates uncertainty and results in substantial wind spillage at higher levels of wind penetration, which lead to the unnecessarily expensive operating cost. However, this formulation results in no load shedding for any wind penetration level.

TABLE IV
STATISTICS OF MONTE CARLO SIMULATIONS FOR DIFFERENT WIND PENETRATION (COSTS ARE IN 10^3, \$)

Wind Penetration	Variable	HUC	SUC	IUC
10 %	$E(C)$	908.7	919.6	977.4
	$EENS$, MWh	0.019	0.34	0
	WS, MWh	33.4	18.5	24.3
20 %	$E(C)$	712.4	727.8	800.1
	$EENS$, MWh	0.023	0.59	0
	WS, MWh	99.6	108.1	214.3
30 %	$E(C)$	654.1	679.7	709.4
	$EENS$, MWh	0.024	0.59	<0.001
	WS, MWh	151.4	152.0	331.2

IV. CONCLUSION

This paper proposes a unit commitment formulation that balances the robustness of the interval unit commitment and the low expected cost of the stochastic unit commitment. Instead of enforcing a uniformly high level of robustness (like the interval unit commitment) or tolerating a certain amount of infeasibility (like the stochastic unit commitment), this hybrid approach optimally decides when a more expensive schedule is justified. A detailed Monte Carlo simulation demonstrates that it always achieves the lowest expected actual operating cost. The schedules produced by this hybrid formulation depend on the $VoLL$, i.e., the value that customers attach to the short-term continuity of supply. As this value increases, the hybrid formulation schedules more resources to reduce the uncertainty that the stochastic unit commitment leaves unhedged.

The proposed HUC assumes a vertically integrated power system, so future work will explore how the proposed formulation could be implemented in a market environment. In particular, future work will focus on studying the impact of switching on an individual producer and customer. The computational performance of the proposed formulation can be increased in the future by implementing a decomposition algorithm and implementing a more efficient parallel computing approach. This is particularly important for the market-based implementation, since the number of decisions to be made will be larger than in the vertically integrated case.

REFERENCES

[1] H. Pandzic, Y. Dvorkin, Y. Wang, T. Qui, and D. S. Kirschen, "Effect of time resolution on unit commitment decisions in systems with high wind penetration," in *Proc. 2014 IEEE Power and Energy Society General Meeting*, 2014, pp. 1–5, accepted for publication.

[2] C. Wang and S. M. Shahidehpour, "Effects of ramp-rate limits on unit commitment and economic dispatch," *IEEE Trans. Power Syst.*, vol. 8, no. 3, pp. 1341–1350, Aug. 1993.

[3] G. Morales-Espana, J. M. Latorre, and A. Ramos, "Tight and compact MILP formulation for the thermal unit commitment problem," *IEEE Trans. Power Syst.*, vol. 28, no. 4, pp. 4897–4908, Nov. 2013.

[4] ISO New England Operating Procedure No. 8 Operating Reserve and Regulation [Online]. Available: http://www.iso-ne.com/rules_proceds/operating/isone/op8/op8_rto_final.pdf

[5] PJM Manual 11. Energy & Ancillary Services Market Operations [Online]. Available: http://www.pjm.com/~/media/documents/manuals/m11.ashx

[6] Y. V. Makarov, C. Loutan, M. Jian, and P. de Mello, "Operational impacts of wind generation on California power systems," *IEEE Trans. Power Syst.*, vol. 24, no. 2, pp. 1039–1050, May 2009.

[7] Y. Dvorkin, M. A. Ortega-Vazquez, and D. S. Kirschen, "Assessing flexibility requirements in power systems," *IET Gener., Transm., Distrib.*, accepted for publication.

[8] M. A. Ortega-Vazquez and D. S. Kirschen, "Should the spinning reserve procurement in systems with wind power generation be deterministic or probabilistic?," in *Proc. Int. Conf. Sustainable Power Generation and Supply*, 2009, pp. 1–9.

[9] W. Lei, M. Shahidehpour, and L. Tao, "Stochastic security-constrained unit commitment," *IEEE Trans. Power Syst.*, vol. 22, no. 2, pp. 800–811, May 2007.

[10] F. Bouffard, F. D. Galiana, and A. J. Conejo, "Market-clearing with stochastic security—part I: Formulation," *IEEE Trans. Power Syst.*, vol. 20, no. 4, pp. 1818–1826, Nov. 2005.
[11] J. Dupacova, N. Growe-Kuska, and W. Romisch, "Scenario reduction in stochastic programming: An approach using probability metrics," *Math. Program.*, vol. 95, pp. 493–511, 2003.
[12] H. Heitsch and W. Romisch, "Scenario reduction algorithms in stochastic programming," *Comput. Optim. Appl.*, vol. 24, no. 2-3, pp. 187–206, 2003.
[13] W. Lei, M. Shahidehpour, and L. Zuyi, "Comparison of scenario-based and interval optimization approaches to stochastic SCUC," *IEEE Trans. Power Syst.*, vol. 27, no. 2, pp. 913–921, May 2012.
[14] Y. Dvorkin, Y. Wang, H. Pandzic, and D. S. Kirschen, "Comparison of scenario reduction techniques for the stochastic unit commitment," in *Proc. 2014 IEEE Power and Energy Society General Meeting*, 2014, pp. 1–5, accepted for publication.
[15] S. M. Ryan, R. J. B. Wets, D. L. Woodruff, C. Silva-Monroy, and J.-P. Watson, "Toward scalable, parallel progressive hedging for stochastic unit commitment," in *Proc. 2013 IEEE Power and Energy Society General Meeting*, 2013, pp. 1–5.
[16] F. Yong, L. Zuyi, and W. Lei, "Modeling and solution of the large-scale security-constrained unit commitment," *IEEE Trans. Power Syst.*, vol. 28, no. 4, pp. 3524–3533, Nov. 2013.
[17] Y. Wang, Q. Xia, and C. Kang, "Unit commitment with volatile node injections by using interval optimization," *IEEE Trans. Power Syst.*, vol. 26, no. 3, pp. 1705–1713, Aug. 2011.
[18] J. W. Chinneck and K. Ramadan, "Linear programming with interval coefficients," *JORS*, vol. 51, no. 2, pp. 209–220, 2000.
[19] D. Bertsimas, E. Litvinov, X. A. Sun, Z. Jinye, and Z. Tongxin, "Adaptive robust optimization for the security constrained unit commitment problem," *IEEE Trans. Power Syst.*, vol. 28, no. 1, pp. 52–63, Feb. 2013.
[20] C. Zhao, J. Wang, J. P. Watson, and Y. Guan, "Multi-stage robust unit commitment considering wind and demand response uncertainties," *IEEE Trans. Power Syst.*, vol. 28, no. 3, pp. 2708–2717, Aug. 2013.
[21] C. Zhao and Y. Guan, "Unified stochastic and robust unit commitment," *IEEE Trans. Power Syst.*, vol. 28, no. 3, pp. 3353–3361, Aug. 2013.
[22] M. A. Ortega-Vazquez and D. S. Kirschen, "Optimizing the spinning reserve requirements using a cost/benefit analysis," *IEEE Trans. Power Syst.*, vol. 22, no. 1, pp. 24–33, Feb. 2007.
[23] J. M. Morales, A. J. Conejo, and J. Perez-Ruiz, "Economic valuation of reserves in power systems with high penetration of wind power," *IEEE Trans. Power Syst.*, vol. 24, no. 2, pp. 900–910, May 2009.
[24] A. J. Conejo, M. Carrion, and J. M. Morales, *Decision Making Under Uncertainty in Electricity Markets*. New York, NY, USA: Springer, 2010.
[25] K. K. Kariuki and R. N. Allan, "Evaluation of reliability worth and value of lost load," *IEE Proc.—Gener., Transm., Distrib.*, vol. 143, no. 2, pp. 171–180, 1996.
[26] R. Baldick, "Wind and energy markets: A case study of texas," *IEEE Syst. J.*, vol. 6, no. 1, pp. 27–34, 2012.
[27] J. G. Deqiang and E. Litvinov, "Energy and reserve market designs with explicit consideration to lost opportunity costs," *IEEE Trans. Power Syst.*, vol. 18, no. 1, pp. 53–59, Feb. 2003.
[28] E. Saiz-Marin, J. Garcia-Gonzalez, J. Barquin, and E. Lobato, "Economic assessment of the participation of wind generation in the secondary regulation market," *IEEE Trans. Power Syst.*, vol. 27, no. 2, pp. 866–874, May 2012.
[29] M. Lange, "Analysis of the uncertainty of wind power predictions," Ph.D. dissertation, Fakultt Mathematik und Naturwissenchaften, Carl von Ossietzky Universitt, Oldenburg, Germany, 2003.
[30] M. Lange, "On the uncertainty of wind power predictions analysis of the forecast accuracy and statistical distribution of errors," *J. Solar Energy Eng.*, vol. 127, no. 2, pp. 177–184, 2005.
[31] D. Rajan and S. Takriti, Minimum Up/Down Polytopes of the Unit Commitment Problem With Start-Up Costs, IBM Research Rep., 2005.
[32] C. K. Simoglou, P. N. Biskas, and A. G. Bakirtzis, "Optimal self-scheduling of a thermal producer in short-term electricity markets by MILP," *IEEE Trans. Power Syst.*, vol. 25, no. 4, pp. 1965–1977, Nov. 2010.
[33] K. Purchala, L. Meeus, D. Van Dommelen, and R. Berlmans, "Usefulness of DC power flow for active power flow analysis," in *Proc. 2005 IEEE Power Engineering Society General Meeting*, 2005, pp. 1–5.
[34] A. Ardakani and F. Bouffard, "Identification of umbrella constraints in DC-based security-constrained optimal power flow," *IEEE Trans. Power Syst.*, vol. 28, no. 4, pp. 3924–3934, Nov. 2013.
[35] B. Stott, J. Jardim, and O. Alsac, "DC power flow revisited," *IEEE Trans. Power Syst.*, vol. 24, no. 3, pp. 1290–1300, Aug. 2009.
[36] R. P. Brent, *Algorithms for Minimization Without Derivatives*. New York, NY, USA: Dover, 1973.
[37] J. Kim, "Iterated grid search algorithm on unimodal criteria," Ph.D. dissertation, Virginia Polytech. Inst. State Univ., Blacksburg, VA, USA, 1997.
[38] H. Pandzic, T. Qiu, and D. S. Kirschen, "Comparison of state-of-the-art transmission constrained unit commitment formulations," in *Proc. 2013 IEEE Power and Energy Society General Meeting*, 2013, pp. 1–5.
[39] ERCOT, Day-Ahead Market Information [Online]. Available: http://www.ercot.com/mktinfo/dam/
[40] A. Papavasiliou and S. S. Oren, "Multiarea stochastic unit commitment for high wind penetration in a transmission constrained network," *Oper. Res.*, vol. 61, no. 3, pp. 578–592, 2013.
[41] A. Greenhall, "Wind scenarios for stochastic energy scheduling," Ph.D. dissertation, Dept. Elect. Eng., Univ. Washington, Seattle, WA, USA, 2013.
[42] G. J. Hahn and S. S. Shapiro, *Statistical Models in Engineering*. New York, NY, USA: Wiley, 1967.
[43] M. A. Ortega-Vazquez and D. S. Kirschen, "Assessing the impact of wind power generation on operating costs," *IEEE Trans. Smart Grid*, vol. 1, no. 3, pp. 295–301, 2010.
[44] M. S. Nazir and F. Bouffard, "Intra-hour wind power characteristics for flexible operations," in *Proc. 2012 IEEE Power and Energy Society General Meeting*, 2012, pp. 1–8.

Yury Dvorkin (S'11) received the B.S.E.E. degree with the highest honors at Moscow Power Engineering Institute (Technical University), Moscow, Russia, in 2011. He is pursuing the Ph.D. degree at the University of Washington, Seattle, WA, USA.

He is a recipient of the Clear Energy Institute's Graduate Fellowship. Currently he is a graduate student intern at the Center for Nonlinear Studies at the Los Alamos National Laboratory. His research interests include operational and long-term flexibility in power systems, decision-making under uncertainty in power systems, power system analysis and operation, and power system economics.

Hrvoje Pandžić (S'06–M'12) received the M.E.E. and Ph.D. degrees from the Faculty of Electrical Engineering, University of Zagreb, Croatia, in 2007 and 2011, respectively.

He is currently a postdoctoral researcher at the University of Washington, Seattle, WA, USA. His research interests include planning, operation, control and economics of power and energy systems.

Miguel A. Ortega-Vazquez (S'97–M'06) received the electrical engineers degree from the Instituto Tecnolgico de Morelia, Mexico, in 1999, the M.Sc. degree from the Universidad Autnoma de Nuevo Len, Mexico, in 2001, and the Ph.D. degree from The University of Manchester (formerly UMIST), Manchester, U.K., in 2006, all with emphasis in power systems.

He was a Research Associate at the School of Electrical and Electronic Engineering at The University of Manchester until 2010 and Assistant Professor at the Department of Energy and Environment at Chalmers University of Technology, Gothenburg, Sweden, until 2011. In 2012 he joined the University of Washington, Seattle, WA, USA, as a Research Assistant Professor. His research interests are in the fields of power systems security, economics, and operation.

Daniel S. Kirschen (M'86–SM'91–F'07) received the electrical and mechanical engineer's degrees from the Université Libre de Bruxelles, Belgium, in 1979, and the M.Sc. and Ph.D. degrees from the University of Wisconsin, Madison, WI, USA, in 1980 and 1985, respectively.

He is currently Close Professor of Electrical Engineering at the University of Washington, Seattle, WA, USA. His research focuses on smart grids, the integration of renewable energy sources in the grid, power system economics and power system security.